FUNDAMENTALS & APPLICATIONS

CHEMELECTROCHEM

ANALYSIS & CATALYSIS, BIO & NANO, ENERGY & MORE

Accepted Article

Title: Silver Nanoparticle/Multi-Walled Carbon Nanotube Hybrid as an Efficient Electrocatalyst for Oxygen Reduction Reaction in Alkaline Medium

Authors: LuLu Guo, Li Xiang, Fujie Li, Xiaoteng Liu, Lei Xing, Degui Li, Zhihong Luo, and Kun Luo

To be cited as: *ChemElectroChem* 10.1002/celc.201900232

Link to VoR: http://dx.doi.org/10.1002/celc.201900232

A Journal of

ChemPubSoc Europe

WILEY-VCH

www.chemelectrochem.org

Silver Nanoparticle/Multi-Walled Carbon Nanotube Hybrid as an Efficient Electrocatalyst for Oxygen Reduction Reaction in Alkaline Medium

LuLu Guo[2#], Li Xiang[2#], Fujie Li[2], Xiaoteng Liu[4], Lei Xing[3], Degui Li[2], Zhihong Luo[2*], Kun Luo[1,2]*

1. School of Materials Science and Engineering, Changzhou University, Changzhou 213164, P R China;

2. College of Materials Science and Engineering, Guilin University of Technology, Guilin 541004, P R China;

3. Institute of Green Chemistry and Chemical Technology, Jiangsu University, Zhenjiang 212013, P R China;

4. Department of Mechanical and Construction Engineering, Northumbria University, Newcastle-upon-Tyne, NE7 7XA, UK.

Abstract

A facile approach is employed to synthesize silver nanoparticle/multi-walled carbon nanotube (Ag/MWNTs) hybrids by the direct reduction of silver nitrate with presence of MWNTs, where Ag nanoparticles capped with tris(hydroxymethyl)phosphine oxide (d = 2.9 nm) are uniformly deposited on MWNTs. The as-synthesized Ag/MWNTs hybrids exhibit high catalytic activity toward oxygen reduction, which increases with the loading amounts of Ag nanoparticles. RDE and RRDE analyses further indicate that the Ag/MWNTs hybrids follow the same four-electron pathway towards oxygen reduction reaction as the Pt/C catalyst, and the Ag/MWNTs hybrid (22.8 wt.%) manifests comparable catalytic activity to the 20% Pt/C catalyst, together with superior long-term stability and methanol tolerance, demonstrating the potential application on direct methanol fuel cells as an effective oxygen reduction catalyst.

Keywords: silver nanoparticle; multi-walled carbon nanotube; electrocatalyst; oxygen reduction reaction; methanol tolerance

 # First authors: L. Guo and L. Xiang. *Corresponding authors: Prof. Kun Luo, email: luokun@cczu.edu.cn; Dr. Zhihong Luo, email: luozhihong615@glut.edu.cn.

1. Introduction

Direct methanol fuel cells (DMFCs) are listed in a subcategory of fuel cells, which generate electricity based on the oxidation of methanol and reduction of oxygen.[1-2] Pt-based catalysts are frequently used to accelerate the sluggish kinetics of oxygen reduction reaction (ORR), but suffer from natural scarcity, high cost, poor durability and obvious poisoning effect by the crossover of methanol, which have become a bottle neck for the large-scale commercialization of DMFCs.[3-4] Massive efforts have been devoted to explore active, cost-effective and stable catalysts, including low platinum loaded catalysts,[5-6] non-Pt noble metals,[7-8] transition metal compounds [9-10] and heteroatom doped carbon materials.[11-12] Non-Pt noble metals like Au and Ag present excellent electric conductivity and chemical stability, but exhibit weaker activity towards ORR due to their filled *d* bands than smooth Pt with partially filled *d* band. However, the catalytic properties of Au and Ag can be significantly enhanced when they are in nanoscale, because the gaps between the *d*-band and the Fermi level of low-coordinated metal atoms are obviously narrowed. Following this context, Au and Ag nanoparticles (NPs) have been reported to manifest impressive ORR catalytic activity and durability in previous literature, [7,13] where the Ag NPs appear more attractive for their low cost and considerable stability in alkaline solution.[14]

The (111) facet of bulk Ag is normally considered to be active for oxygen reduction, which occurs via a direct four-electron ($4e^-$) pathway in alkaline media.[15] As the size reduces to nanometers, the catalytic performance of Ag towards ORR is also changed. Narayanamoorthy et al. synthesized Ag nanoflowers with the petal length of 180-300 nm and thickness of ca.15 nm, which manifested high catalytic activity with the total electron transfer number of 4.1.[16] However, Garcia et al. reported that round Ag NPs (20 nm) protected by poly(vinyl pyrrolidone) on carbon substrate only involved in a $2.7e^-$ exchange for the reduction of oxygen but still preserved considerable catalytic activity.[17] Jin et al. demonstrated that the Ag NPs (2 nm) protected with single-stranded oligonucleotide sequence (ssDNA) exhibited a $3.5e^-$ pathway towards ORR with excellent stability.[18] Lu et al. illustrated that the Ag

nanoclusters (0.7 nm) protected by meso-2,3-dimercapto-succinic acid followed a 2.3e^- pathway, while the Ag NPs (3.3 nm) with the same capping ligand proceeded with a 2.8e^- ORR process, however, the former still manifested higher activity than the latter in alkaline electrolytes.[19] Soo et al. noticed that the electron transfer number varied from 2 to 4 when nitrogen-doped graphene replaced graphene as substrate.[20] Similarly, Cao et al. also indicated that the catalytic activity of Ag/C was effectively enhanced when Ŭ-MoC was deposited onto carbon substrate, and the reason was assigned to the homogeneous distribution of ultrafine Ag NPs facilitated by Ŭ-MoC.[21] Interestingly, Cheng et al. reported that the electron transfer number could be increased from 3 to 4 accompanied with enhanced catalytic activity, when the loading amount of Ag NPs raised from 20 wt.% to 50 wt.%.[22] Xu et al. dramatically increased the loading amounts of Ag from 40 wt.% to 392 wt.%, and the H_2O_2 yield (corresponding to the 2e^- ORR pathway) was observed to decline from 15% to less than 5%.[23] The above investigations suggests that the ORR of Ag NPs is a complicated process, which is likely involved in the Ag particle size, crystal structure, surface chemistry and interaction with supporting substrates. Therefore, more investigations are still needed for further understanding on the catalytic mechanism of Ag NPs.

Herein, we present a facile approach to synthesize Ag NPs (2.9 nm) and multi-walled carbon nanotubes hybrids (Ag/MWNTs) via the reduction of silver nitrate by tetrakis(hydroxylmethyl)phosphonium chloride (THPC) with the presence of MWNTs. The Ag/MWNTs hybrids manifest excellent catalytic activity following a direct 4e^- pathway towards ORR, together with superior durability and methanol tolerance in comparison with the commercial Pt/C catalyst.

2. Experimental Section

2.1 Chemicals and Materials

Multi-walled carbon nanotubes (MWNTs, 10 nm × 3~6 ㎜, Sigma), hydrogen peroxide (H_2O_2, 35% aqueous solution, Xilong Chemical Co. Ltd.), 20 wt.% Pt/C catalysts (Alfa Aesar), silver nitrate (Sinopharm Chemical

Reagent Co. Ltd), tetrakis(hydroxylmethyl)phosphonium chloride (THPC, 80% aqueous solution, Tokyo Chemical Industry Co. Ltd.), potassium hydroxide (KOH, AR, Xilong Chemicals Co. Ltd) and Nafion solution (5%, Sigma-Aldrich) were directly used without further treatment. Deionized water (18.2 MΩcm) was employed in the experiments.

2.2 Synthesis of Ag/MWNTs hybrids

A moderate surface oxidation was applied on the MWNTs in advance to improve the affinity with water before loading Ag NPs, following a method introduced in our previous work.[7] Typically, MWNTs (1.0 g) powders were added into a gas-proof Erlenmeyer flask connected with a separation funnel (with 100 mL of H_2O_2) and a pipe to a vacuum pump. The flask was evacuated at a pressure of 0.01 MPa for 10 min, and then was vented by allowing the addition of H_2O_2 in the funnel into the lower Erlenmeyer flask. The suspension was stirred for 2 h and then allowed to stay overnight. The MWNTs in the suspension were separated and rinsed for three times with deionized water by centrifuging at 8000 rpm, and were dried in an oven at 80 ^{o}C overnight.

50 mg of the oxidized MWNTs were added in 100 mL of 2 mM $AgNO_3$ and kept stirring for 2 h. Then, 1.0 M KOH solution was employed to adjust the pH of the suspension to 12.3, followed with the addition of 5 mL of 50 mM THPC solution. The suspension was continued stirring for 2 h and then left overnight. The precipitate was separated and repeatedly rinsed with deionized water by centrifuging at 8000 rpm till the supernatant was neutral. Then, the precipitate was removed to dry at 80 ^{o}C in an oven, led to the Ag/MWNTs hybrids. The loading amounts of Ag NPs were varied by altering the mass of MWNTs in the system, where 32.4 mg and 86.4 mg of MWNTs were used for comparison.

2.3 Characterizations

The morphology of the Ag/MWNTs catalysts was characterized by a Spherical Aberration Corrected Field Emission Transmission Electron Microscope (Titan G2 60-300) operating at 200 kV. The structure of Ag/MWNTs

catalysts were detected by an X-ray diffractometer (XRD, XôPert PRO) with Cu kα radiation. The surface chemistry of the Ag/MWNTs hybrids was analyzed by Fourier transmittance infrared spectroscopy (FT-IR, Thermo Nexus 470) and X-ray photoelectron spectroscopy (XPS, ESCALAB 250Xi, Thermo Fisher Scientific) using Al KŮ as a source. The Ag loading mass of the Ag/MWNTs hybrids was estimated by a thermogravimetric analyzer (TA instruments, TGA Q500) at a heating rate of 10 ^{o}C min^{-1} in O_2 atmosphere, where the amounts of Ag NPs in the hybrids were calculated by its molar content in the resulted Ag_2O residual at 1000 ^{o}C.

Voltammetric analysis was carried out by an electrochemical workstation (CHI660E, CH Instruments), and electrochemical impedance spectroscopy (EIS) analysis was performed by an electrochemical workstation (CHI 750E, CH Instrument), where a glassy carbon electrode (S = 0.126 cm^2), a platinum wire and a Ag/AgCl electrode were employed as the working, counter and reference electrodes, respectively. The catalyst slurry was prepared by blending 4 mg of the Ag/MWNTs hybrid, 100 εL of Nafion solution, 1.0 mL mixture of ethanol and deionized water (at the volume ratio of 1 : 4) under ultrasonic stirring for 30 min. 8 εL of the slurry was dropped onto the GC electrode, which was used as the modified electrode for the both electrochemical experiments. Typically, CV curves were measured at the scan rate of 20 mV s^{-1} in N_2 or O_2 saturated 0.1 M KOH solutions, respectively, and EIS spectra were recorded at the open circuit potential with 5 mV of AC amplitude in the frequency range from 0.1 Hz to 1 MHz in 0.1 M KOH electrolytes.

Investigations on the ORR kinetics of the hybrids were carried out by using a rotating disk electrode (RRDE-3A, ALS Co. Ltd) ranging from 0.1 V to -0.6 V (vs. Ag/AgCl) at a scan rate of 5 mV s^{-1}, where a GC rotating disk electrode (RDE, 0.07 cm^2) and a rotating ring-disk electrode (RRDE) equipped with a GC disk (0.126 cm^2) and a Pt ring (0.189 cm^2) were employed in the experiments. 5 εL and 8 εL of the catalyst slurries were used to modify the GC electrodes of the RDE and RRDE, respectively, and the linear sweep voltammetric (LSV) profiles were recorded in O_2-saturated 0.1 M KOH solutions.

3. Results and Discussion

3.1 Morphology and surface chemistry

The TEM image shown in Fig. 1a illustrates that the dark nanoparticles (Ag NPs) are well dispersed on the MWNTs surface, where the HRTEM micrograph in the upper inset of Fig.1a suggests that the Ag NPs are actually nanocrystals with a lattice spacing of 0.238 nm, corresponding to the (111) facet of Ag crystal. The average particle size is measured as 2.9 ± 0.1 nm (N=200) as displayed in the lower inset of Fig.1a. Some larger particles are examined under HRTEM, Fig. S1 in the Supporting Information illustrates that about eight Ag nanoparticles are seen around the MWNTs within the scope of 20 nm, demonstrating that the large particle is actually the aggregate of a few Ag nanoparticles. The thermogravimetric analysis of the Ag/MWNTs hybrids in Fig.1b displays that the three samples with different Ag loading amounts remain stable at the temperature lower than 400 ^{o}C. The decomposition starts from ca. 530 ^{o}C, leaving the residual amounts of 34.7 wt.%, 24.5 wt.% and 17.9 wt.% for the three samples at 1000 ^{o}C, respectively. The loading amounts of Ag NPs are therefore calculated as 32.3 wt.%, 22.8 wt.% and 16.6 wt.% according to the content of Ag in Ag_2O.

Fig. 1c compares the XRD patterns of the Ag/MWNTs hybrids with the Ag loading amounts of 16.8%, 22.8% and 32.3%. It is seen that four common peaks appeared at 37.9 °, 44.1 °, 64.6 ° and 77.5 ° for the three samples, assigned to the (111), (200), (220) and (311) facets of Ag crystal (JCPDF No. 01-1164). The peak at 26.4 ° is also present in the curves for the three samples, which is attributed to the (002) facet of graphite sheets of MWNTs (JCPDF No. 25-0284). Moreover, the intensity of the Ag peaks appears to increase with the Ag loading amounts, while the strength of the MWNTs peak keeps basically unchanged.

Fig.1d illustrates that the FTIR spectra of the three Ag/MWNTs hybrids present the identical features. Two peaks occur at 3431 cm^{-1} and 1633 cm^{-1} attributed to the stretching and deformation vibrations of -OH group, and the three bands at 2973 cm^{-1}, 2917 cm^{-1} and 1397 cm^{-1} can be assigned to the asymmetrical stretching, symmetrical

stretching and bending vibrations of -CH_2. The peak at 1101 cm^{-1} is attributed to P=O stretching vibration.[7] The results suggest that the capping agent on the Ag NPs is likely tris(hydroxymethyl)phosphineoxide (THPO).

The surface chemistry of the Ag/MWNTs hybrid was also investigated by XPS analysis. The C_{1s} spectrum displayed in Fig.2a resolves in three peaks at 284.8 eV, 285.1 eV and 286.0 eV, corresponding to C-H/C-C, C-P and C-OH groups, respectively. The fitting of the high-resolution P_{2p} signal results in three peaks in Fig.2b at 132.9 eV, 133.8 eV and 134.6 eV, indicating the existence of P-C, P=O and P-Ag bands, respectively. The resolved Ag_{3d} signal in Fig.2c presents a pair of fitting peaks at 374.7 eV and 368.7 eV, corresponding to the $Ag_{3d3/2}$ and $Ag_{3d5/2}$. The above results are listed in Table 1, from which the atomic ratio of C-OH (25.1 at.%) to C-P (24.32 at.%) is approximate 1, and the ratio among the percentages of P-C (59.9 at.%), P=O (19.97 at.%) and P-Ag (20.13 at.%) is approximate 3:1:1, indicating that THPO is the capping agent on the Ag NPs, in agreement with the FTIR analysis. It was reported that the cleavage of THPC in alkaline solution generates the products of THPO, formaldehyde and small amount of tris(hydroxymethyl)phosphine (THP), where the unstable THP can be shortly oxidized to THPO in air.[24] Therefore, it is reasonable that THPO serves as the capping ligand of the as-synthesized Ag NPs in alkaline media.

3.2 Catalytic activity towards ORR

The CV scans of the Ag/MWNTs hybrids are compared with the pristine MWNTs in both O_2 and N_2 saturated 0.1 M KOH solutions as displayed in Fig.3. As reference, no reduction peak is seen in the four CV curves (black lines) in the N_2-saturated KOH solutions, indicating that no ORR occurs, and the MWNTs and Ag/MWNTs hybrids remain stable ranging from 0.2 V to -0.6 V (vs. Ag/AgCl). In O_2-saturated electrolytes, strong reduction peaks are measured (red lines) at -0.239 V, -0.246 V and -0.242 V for the 16.6% (Fig.3a), 22.8% (Fig.3b) and 32.3% (Fig.3c) Ag/MWNTs hybrids, with the corresponding peak current densities at 0.507 mA cm^{-2}, 0.552 mA cm^{-2} and 0.628 mA cm^{-2}, respectively. In Fig.3d, the reduction peak appears at -0.264 V for the pristine MWNTs with a current density

10.1002/celc.201900232

of only 0.241 $mAcm^{-2}$. The EIS analysis shown in Fig.S2 in the Supporting Information displays that the impedance values of electron transfer at high frequency are all small for the Ag/MWNTs hybrids (16.6%, 22.8% and 32.2%), which are benefit for the enhancement of ORR kinetics. The above results demonstrate that the increase of Ag loading brings with the apparent increment of current density for the Ag/MWNTs hybrids, but the peak potential varies slightly. The surface area can also be estimated from the CV plots by using Randles-Sevcik equation, where the values for the pristine MWNTs, 16.6% Ag/MWNTs, 22.8% Ag/MWNTs and 32.3% Ag/MWNTs hybrids are determined as 151.6 cm^2, 318.9 cm^2, 347.2 cm^2 and 395.0 cm^2, respectively.

Linear sweep voltammograms (LSV) of the Ag/MWNTs hybrid modified RDEs were measured in the O_2-saturated 0.1 M KOH solutions at the rotating rates of 400 rpm, 625 rpm, 900 rpm, 1225 rpm, 1600 rpm, 2025 rpm and 2500 rpm, respectively, and the results are displayed in Fig.4a, 4c and 4e. The onset (E_{onset}) and half-wave ($E_{1/2}$) potentials are defined as the potentials at 5% and 50% of the diffusion-limited current, respectively, which are frequently used to characterize the ORR catalytic activity. In this experiment, the E_{onset} and $E_{1/2}$ values at 1600 rpm are determined as -0.15 V and -0.242 V for the 16.6% Ag/MWNTs hybrid, -0.158 V and -0.261 V for the 22.8% Ag/MWNTs hybrid, and -0.160 V and -0.263 V for the 32.3% Ag/MWNTs hybrid. Correspondingly, the limiting current densities for the three samples are measured as 4.37 mA cm^{-2}, 5.24 mA cm^{-2} and 5.51 mA cm^{-2}, respectively. It is clear that the diffusion-limited current density increases with the Ag loading amount, suggestive of the improvement on ORR kinetics in line with the CV results.

ORR occurs in alkaline solution media normally following any one of the below pathways:[25]

$O_2 + 2H_2O + 4e^- \rightarrow 4OH^-$ (Direct $4e^-$ pathway) (1)

$O_2 + H_2O + 2e^- \rightarrow HO_2^- + OH^-$ ($2e^-$ pathway) (2)

$HO_2^- + H_2O + 2e^- \rightarrow 3OH^-$ (Subsequential $4e^-$ pathway) (3)

Koutecky-Levich (K-L) plots are used to determine the pathway of ORR process, where the reciprocal of

 10.1002/celc.201900232

current density (J^{-1}) is used as a function of the inverse square root of the rotating rate ($ɤ^{-1/2}$), and the overall electron transfer numbers (n) can be calculated by the following equations:

*٩٠ سي ٌ٩٠ طى ŏ| ٩٠٧٠ (4)

" سي π8ς Î&!#ļ Ó ļ ·٧١ ، ٩٠٧۴ (5)

where J is the measured current density, J_k is the kinetic current density, ω is the angular velocity of the disk (rpm), F is the Faraday constant (96485 C mol^{-1}), C_O (1.2×10^{-6}mol cm^{-3}) is the bulk concentration of O_2 in the electrolyte, D_O (1.9×10^{-5} cm^2 s^{-1}) is the diffusion coefficient, and ս (0.01 cm^2 s^{-1}) is the kinetic viscosity of the electrolyte. The n values of the 16.6% Ag/MWNTs, 22.8% Ag/MWNTs and 32.3% Ag/MWNTs hybrids are calculated as 3.6, 4.2 and 4.3 shown in Fig.4b, 4d and 4f, respectively, indicative of the $4e^-$ pathway towards ORR in alkaline media.

RRDE analysis was also used to study the oxygen reduction kinetics of the Ag/MWNTs hybrids, where the potential of the disk electrode swept from 0 V to -0.6 V, and the ring electrode was settled at 0.8 V. The electron transfer number n and corresponding H_2O_2 yield are calculated by using the following equations:

ἐ سي ٢عيٳش / ٳش٨ ٳها٧إ (6)

Ő. ǘ. Þ سي ςππ عي ٳها٧إ / ٳش٨ ٳها٧إ Þ (7)

where I_d is the disk current (A), I_r is the ring current (A), N ($=I_r/I_d$, collection efficiency) is taken as 44% according to our previous work.[7] As illustrated in Fig.5a, the disk current (black line) modified with the 16.6% Ag/MWNTs hybrid increases with the overpotential, which ends up with a platform due to the limited current by the diffusion of oxygen. The ring current (red line) in association with H_2O_2 oxidation gradually approaches to zero as the potential varies from -0.15 V to -0.6 V. The overall electron transfer number n (black line) increases from 3.73 to 3.91, and the H_2O_2 yield (blue line) declines from 13.23% to 4.45% (Fig. 5b). The 22.8% and 32.3% Ag/MWNTs hybrids manifest the similar profiles of the disk and ring currents as shown in Fig.5c and 5e, and the

electron transfer number for the 22.8% Ag/MWNTs hybrid swiftly raises from 3.68 to 3.95 in the range from -0.15 V to -0.6 V as displayed in Fig.5d, in association with the decrease of H_2O_2 yield from 15.75% to 2.69%. In comparison, the *n* value of the 32.3% Ag/MWNTs hybrid climbs up from 3.39 to 3.95 as the disk potential scanned from -0.15 V to -0.6 V (see Fig.6f), leaving less than 2.67% of H_2O_2 yield in the end. The RRDE analysis again demonstrates that the ORR on the Ag/MWNTs hybrids follows the $4e^-$ pathway, in agreement with the RDE analysis. The increase of Ag NPs loading reduces the H_2O_2 yield, suggesting that the $4e^-$ pathway is probably attributed to the Ag NPs on the hybrids.

The ORR catalytic activity of the Ag/MWNTs hybrids was also compared with the commercial 20% Pt/C catalyst by the LSV curves at 1600 rpm. It is seen in Fig. 6a that the $E_{1/2}$ values for the 16.6 % Ag/MWNTs (-0.242 V), 22.8% Ag/MWNTs (-0.261 V) and 32.3% Ag/MWNTs (-0.263 V) hybrids are all negative than the 20% Pt/C catalyst (-0.12 V). As for the limiting current, the 22.8% Ag/MWNTs hybrid exhibits a comparable limited current density to the 20% Pt/C catalyst, while that for the 32.3% Ag/MWNTs hybrid is even larger. Additionally, the Tafel slopes are also plotted to compare the ORR kinetics (Fig.6b), where the values for the 16.6 %, 22.8% and 32.3% Ag/MWNTs hybrids are determined as 71 mV dec^{-1}, 81 mV dec^{-1} and 83 mV dec^{-1}, while the slope for the 20% Pt/C catalyst is measured as 81 mV dec^{-1}. The results suggest that the Ag/MWNTs hybrid with similar catalyst loading (22.8%) exhibits comparable ORR kinetics to the 20% Pt/C catalyst, and the increase of Ag NP loading (32.3%) leads to a larger catalytic current towards ORR.

3.3 Durability and methanol tolerance

Durability is a critical feature for ORR catalysts. In the experiment, the accelerated durability test (ADT) was used to compare the 22.8% Ag/MWNTs and the 20% Pt/C catalyst at a scan rate of 20 mV s^{-1} in O_2-saturated 0.1 M KOH solutions, during which the 1^{st}, 1000^{th}, 2000^{th} and 3000^{th} LSV scans at 1600 rpm were plotted. For the 22.8% Ag/MWNTs hybrid, the $E_{1/2}$ displays a positive shift of 3 mV after 3000 scans in Fig. 7a, accompanied with 12%

current loss. In contrast, the 20% Pt/C catalyst manifests a negative $E_{1/2}$ shift of 9 mV after 3000 scans in Fig. 7b, and the current loss is 14%. It is noticed that the average size of Ag NPs on the 22.8% Ag/MWNTs hybrid increases to 3.8 nm after 3000 LSV scans (shown in Fig. S3 in the Supporting Information), in correspondence to the degradation of ORR kinetics depicted in Fig.7a, suggesting that the size of Ag nanoparticles exerts important effect on the ORR performance of the hybrids.

The methanol tolerance is also of importance for the ORR catalysts applied on DMFCs, because the crossover of methanol through the membrane is hard to avoid in practice. The amperometric measurement was performed at the potential of -0.6 V in O_2-saturated 0.1 M KOH solutions, in order to compare the methanol tolerance of the 22.8% Ag/MWNTs hybrid and the 20% Pt/C catalyst. As shown in Fig.8a, a sharp drop followed with obvious current decay is observed for the 20% Pt/C catalyst in response to the addition of methanol in the system, where only 28.9% of the reduction current is retained after 1300 s. On the other hand, the addition of methanol just causes a current fluctuation for the 22.8% Ag/MWNTs hybrid, and up to 86% of the ORR current is remained after 1300 s of reaction as displayed in Fig. 8b. The above results illustrate that the 22.8% Ag/MWNTs hybrid exhibits superior durability and methanol tolerance over the commercial 20% Pt/C catalyst, which is a promising candidate as ORR catalyst for DMFCs.

4. Conclusion

A facile approach to synthesize the Au/MWNTs hybrids is present by the direct reduction of $AgNO_3$ by THPC in alkaline media, where well-dispersed Ag NPs (d= 2.9 nm) capped with THPO were deposited on the MWNTs substrate. The ORR kinetics of the Ag/MWNTs hybrids increases with the loading amounts of Ag NPs, where the hybrid with similar content of catalyst (22.8 wt.% Ag) manifests comparable ORR catalytic activity to the 20% Pt/C catalyst, together with superior long-term stability and methanol tolerance. RDE and RRDE analyses indicate that the Ag/MWNTs hybrids follow the same four-electron pathway as the Pt/C catalyst, in favor of membrane

protection. The results demonstrate that the Ag/MWNTs hybrid is prospective to serve as an effective ORR catalyst in DMFCs at low cost.

Acknowledgement

The authors appreciate the financial support by the National Natural Science Foundation of China (No. 51874051) and Guangxi Natural Science Foundation (No. 2018GXNSFAA281184 and 2016GXNSFAA380107).

Reference

[1] K. Scott, L. Xing in *Advances in Chemical Engineering Vol. 41* (Ed.: K. Sundmacher), Elsevier, Amsterdam, **2012**, pp. 145-197.

[2] Q. Xu, W. Zhang, J. Zhao, L. Xing, Q. Ma, L. Xu, H. Su H, *Int. J. Green. Energy* **2018**, 15, 181-188.

[3] Y. Sun, L. Xing, K. Scott, *J. Power. Sources* **2010**, 195, 1-10.

[4] M. H. Shao, Q. W. Chang, J. P. Dodelet, R Chenitz, *Chem. Rev.* **2016**, 116, 3594-3657.

[5] S. J. Guo, S. H. Sun, *J. Am. Chem. Soc.* **2012**, 134, 2492-2495.

[6] J. F. Chang, L. G. Feng, K. Jiang, H. G. Xue, W. B. Cai, C. P. Liu, W. Xing, *J. Mater. Chem. A* **2016**, 4, 18607-18613.

[7] L. Xiang, Z. H. Luo, C. L. Hu, Z. C. Cheng, J. W. Lu, Y. C. Cao, K. Luo, *ChemElectroChem* **2018**, 5, 1073-1079.

[8] Y. M. Lee, J. Suntivich, K. J. May, J. E. E. Perry, Y. S. Horn, *Phys. Chem. Lett.* **2012**, 3, 399-404.

[9] A. Aijaz, J. Masa, C. Rösler, W. Xia, P. Weide, A. J. R. Botz, R. A. Fischer, W. Schuhmann, M. Muhler, *Angew. Chem. Int. Ed.* **2016**, 55, 4087-4091.

[10] Y. L. Liu, F. J. Chen, W. Ye, M. Zeng, N. Han, F. P. Zhao, X. X. Wang, Y. G. Li, *Adv. Funct. Mater.* **2017**, 27, 1606034.

[11] D. H. Guo, R. Shibuya, C. Akiba, S. Saji, T. Kondo, J. Nakamura, *Science* **2016**, 351, 361-365.

[12] T. V. Tam, S. G. Kang, K. F. Babu, E. S. Oh, S. G. Lee, W. M. Choi, *J. Mater. Chem. A* **2017**, 5, 10537-10543.

[13] S. Yasmin, M. Ahmed, S. Jeon, *Int. J. Hydrogen Energy* **2017**, 42, 1075-1084.

[14] A. Qaseem, F. Y. Chen, X. Q. Wu, *Catal. Sci. Technol.* **2016**, 6, 3317-3340.

[15] B. B. Blizanac, P. N. Ross, N. M. Markovic, *Electrochim. Acta* **2007**, 52, 2264-2271.

[16] B. Narayanamoorthy, N. Panneerselvam, C. Sita, S. Pasupathi, S. Balaji, I. S. Moon, *J. Electrochem. Soc.* **2016**, 163, H313-H320.

[17] A. C. Garcia, L. H. S. Gasparotto, J. F. Gomes, *Electrocatal.* **2012**, 3, 147-152.

[18] S. Jin, M. Chen, H. F. Dong, B. Y. He, L. Su, W. H. Dai, Q. C. Zhang, X. J. Zhang, *J. Power. Sources* **2015**, 274, 1173-1179.

[19] Y. Z. Lu, W. Chen, *J. Power. Sources* **2012**, 197, 107-110.

[20] L. T. Soo, K. S. Loh, A. B. Mohamad, W. R. W. Daud, W. Y. Wong, *J. Power. Sources* **2016**, 324, 412-420.

[21] L. J. Cao, P. P. Tao, M. C. Li, F. C. Lyu, Z. Y. Wang, S. S. Wu, W. X. Wang, Y. F. Huo, L. Huang, Z. G. Lu, *J. Phys. Chem. Lett.* **2018**, 9, 779-784.

[22] Y. H. Cheng, Y. Y. Tian, S. W. Tsang, C. W. Yan, *Electrochim. Acta* **2015**, 174, 919-924.

[23] X. H. Xu, C. Tan, H. J. Liu, F. Wang, Z. L. Li, J. J. Liu, J. Ji, *J. Electroanal. Chem.* **2013**, 696, 9-14.

[24] K. Luo, S. L. M. Schroeder, R. A. W. Dryfe, *Chem. Mater.* **2009**, 21, 4172-4183.

[25] X. M. Ge, A Sumboja, D. Wuu, T. An, B. Li, F. W. T Goh, T. S. A. Hor, Y. Zong, Z. L. Liu, *ACS. Catal.* **2015**, 5, 4643-4667.

Table 1 Surface chemistry of the 22.8% Ag/MWNTs hybrid by XPS analysis

Elements	Atomic ratio (%)	BE(eV)	Possible chemistry	Component percentage (%)
C_{1s}	89.39	286	C-OH	25.10
		285.1	C-P	24.32
		284.8	C-C/C-H	50.58
P_{2p}	0.18	134.6	Au-P	20.13
		133.8	P=O	19.97
		132.9	P-C	59.9
Ag_{3d}	10.43	374.7	$Ag^{0}_{3d3/2}$	39.34
		368.7	$Ag^{0}_{3d5/2}$	60.66

Figure Captions

Fig. 1 Characterizations of the Ag/MWNTs hybrids with different Ag loading amounts: a-TEM image of the 22.8% Ag/MWNTs hybrid, upper inset: HRTEM image of individual Ag NPs; lower inset: size distribution of Ag NPs; b-TGA curves in O_2 atmosphere; c-XRD spectra; d- FT-IR curves.

Fig. 2 Fitting of the resolved C_{1s} (a), P_{2p} (b) and Ag_{3d} (c) signals of the 22.8% Ag/MWNTs hybrid.

Fig. 3 CV curves of the 16.6% Ag/MWNTs (a), 22.8% Ag/MWNTs (b), 32.3% Ag/MWNTs (c) and pristine MWNTs (d) in N_2 and O_2 saturated 0.1 M KOH.

Fig. 4 RDE polarization curves and corresponding Koutecky-Levich plots for the 16.6% (a, b), 22.8% (c, d), 32.3% (e, f) Ag/MWNTs hybrids.

Fig. 5 RRDE polarization curves and peroxide percentages in ORR catalyzed by the 16.6% (a, b), 22.8% (c, d) and 32.3% Ag/MWNTs hybrids (e, f).

Fig. 6 LSV curves (a) and Tafel plots (b) for the 16.6%, 22.8% and 32.3% Ag/MWNTs hybrids and the 20% Pt/C catalyst.

Fig. 7 Accelerated durability test for the 22.8 % Ag/MWNTs hybrid (a) and the 20% Pt/C catalyst (b) at a scan rate of 20 mV s^{-1} in O_2-saturated 0.1 M KOH solutions. Dash lines mark the $E_{1/2}$ shifts from the 1^{st} scan to 3000^{th} scan.

Fig. 8 Chronoamperometric curves of the 20% Pt/C catalyst (a) and the 22.8% Ag/MWNTs hybrid (b) in O_2-saturated 0.1 M KOH solutions with addition of 3 M methanol solution.

10.1002/celc.201900232

Fig. 1

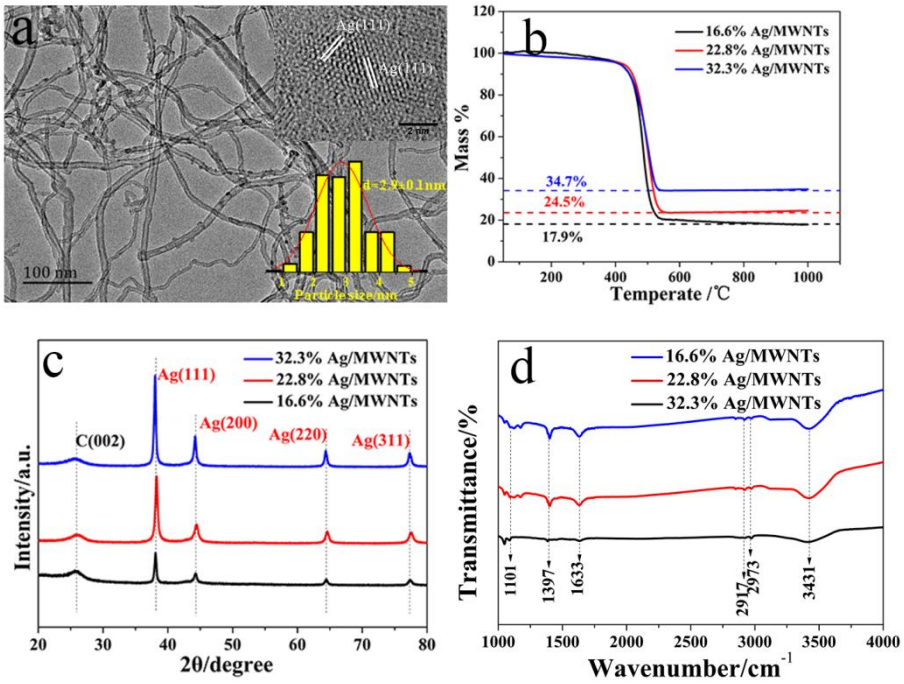

Fig. 2

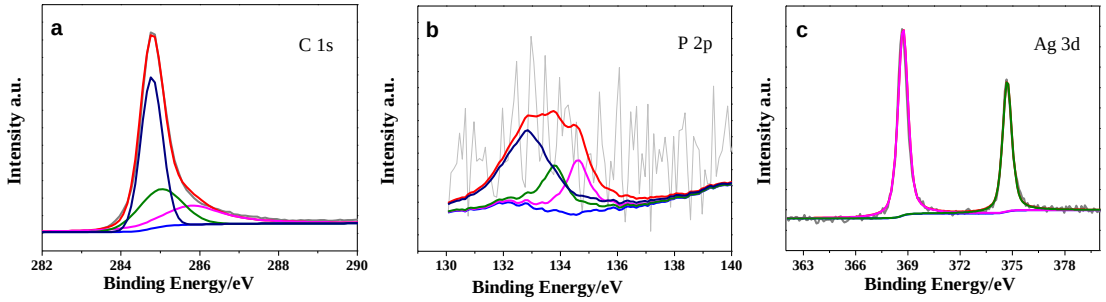

10.1002/celc.201900232

Fig. 3

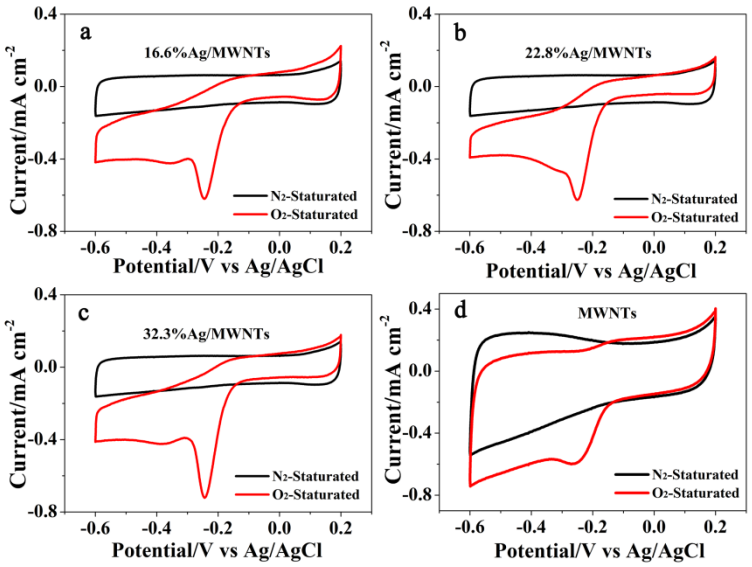

Fig. 4

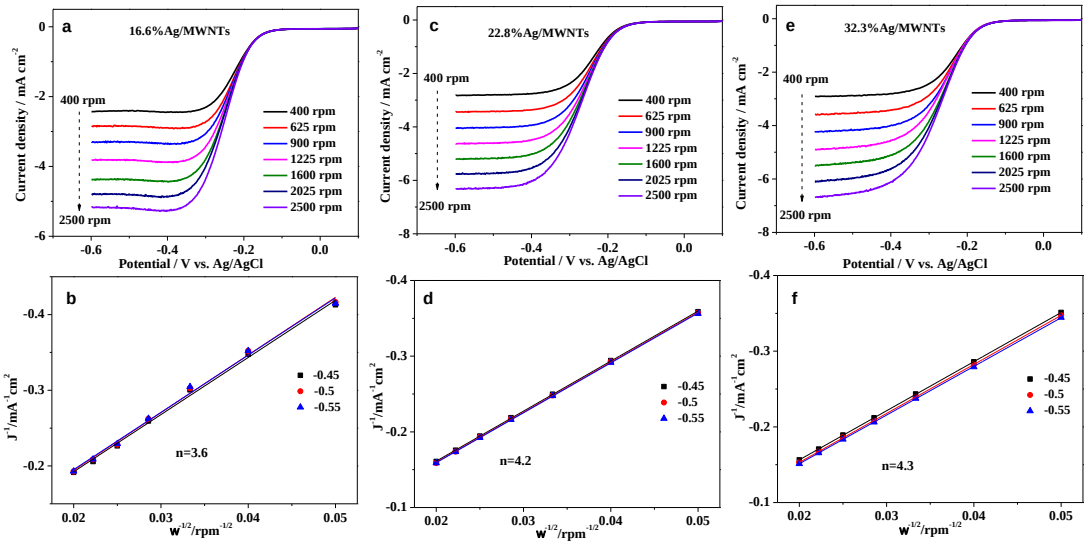

10.1002/celc.201900232

Fig. 5

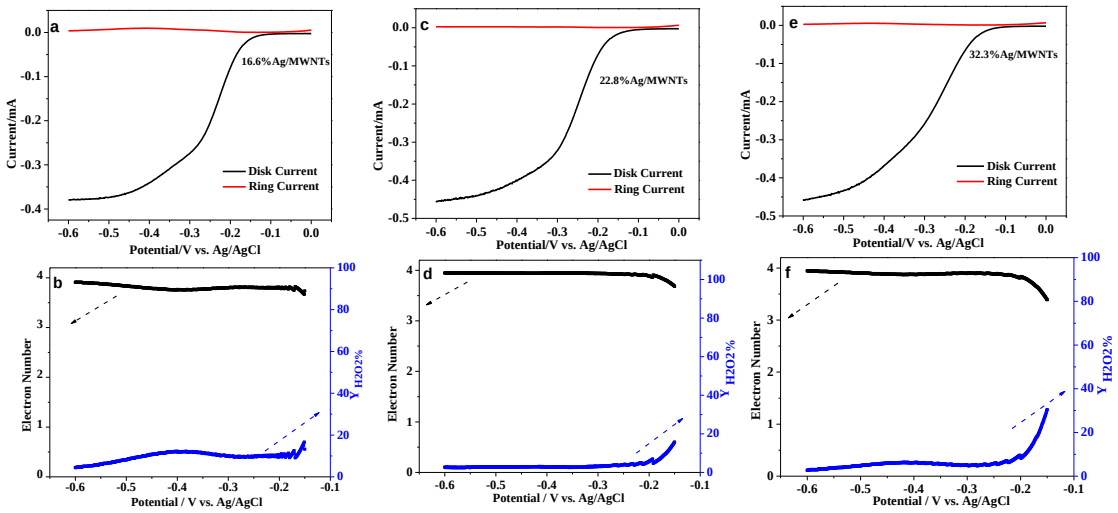

Fig. 6

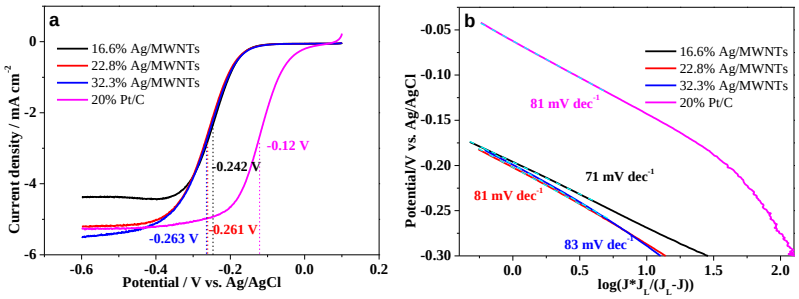

Fig. 7

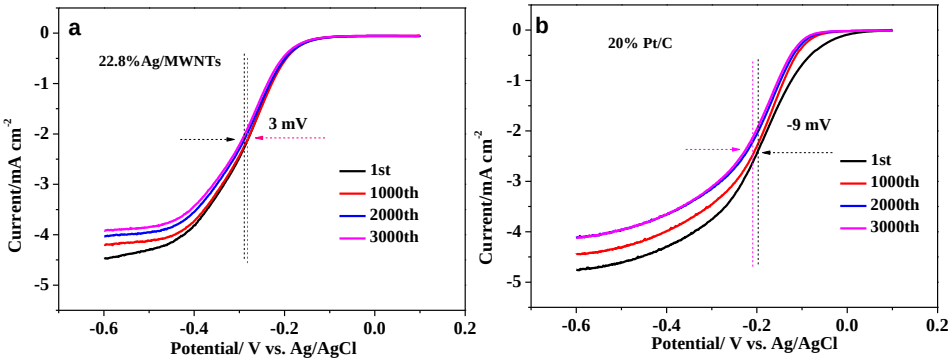

10.1002/celc.201900232

Fig. 8